Time Domain Measurement of Magnetization Dynamics in Ferrofluids

Doctoral Dissertation Defense

Brian Egenriether

Jan 2021

UNIVERSITY OF SOUTH CAROLINA

Agenda

- Introduction and purpose
- Experimental objectives
- Brief theoretical review of magnetization dynamics
- Ferrofluid channel on waveguide
- Inductive technique description
- Experiment descriptions and diagrams
- Measured data and FFTs of time-domain signals
- Introduce FDTD model using Vinamax
- Analysis and discussions
- Questions

UNIVERSITY OF SOUTH CAROLINA

Introduction and Purpose

- Magnetic nanoparticles in colloidal suspension (*ferrofluid*) composed of magnetite (Fe_3O_4) with 10nm diameters (nominal) are studied.
- Similar particles are used in *in vivo* medical imaging, magnetic sensors, drug delivery, cancer research, etc.
- In practically all of these applications, the particles interact with fluctuating magnetic fields and in most cases are still in liquid suspensions.
- Frequency-domain research has been done on ferrofluids, however no time-domain research exists. This may be due to the smallness of the particles, difficulty of dealing with liquid suspensions, and the high speed of the process (~2ns).
- Having an idea of how ferrofluids behave in the time domain yields a better understanding of how to employ them in practice and promotes the scientific field of inquiry.

Experimental Objectives

- To trap ferrofluid above a coplanar waveguide in a sealed channel over the center trace to make time domain measurements of the magnetization dynamics.
- To verify that ferrofluid suspensions undergo the precession dynamics predicted by the Landau-Lifshitz (LL) theory and if these time-domain dynamics can be measured by a magnetic induction technique to be described.
- Perform a fast Fourier transform (FFT) on the data to obtain the frequency response as a function of an external bias field for comparison to other works.
- Derive the effective field of a typical particle in a chain structure and see if resonances in this regime are observed as predicted by the Kittel equation for ferromagnetic spheres.

UNIVERSITY OF SOUTH CAROLINA

Experimental Objectives (cont.)

- Create computer simulations (FDTD) of the time-domain response of interacting free particles, chains of particles and other configurations to the same magnetic field conditions in the experiment.
- Compare the simulation results to the observed waveforms to determine the physical arrangement of constituent nanoparticles. Refine the particle arrangements to best fit the data.
- Study the amplitudes of the FFT to determine how the effective field affects the different components of the response.
- Perform FFT on magnetization dynamics of model to qualitatively observe which fraction of the particles are responsible for each response. Compare to frequency-normalized measured FFT.

Experimental Objectives (cont.)

- Determine the extent to which the particles form chains and observe through modeling the data if they increase in number under increasing fields.
- Determine the approximate (average) coating thickness from chain model.
- Determine distances between chains and see how they change with increasing fields.
- Determine if any higher anisotropy effects are observed and attempt to explain the origin within the framework of the current state of the art.

Landau-Lifshitz Theory

$$\frac{d\vec{\boldsymbol{m}}}{dt} = -\frac{\gamma}{1+\alpha^2}\mu_0\vec{\boldsymbol{m}} \times [\vec{\boldsymbol{H}} + \alpha(\vec{\boldsymbol{m}} \times \vec{\boldsymbol{H}})]$$

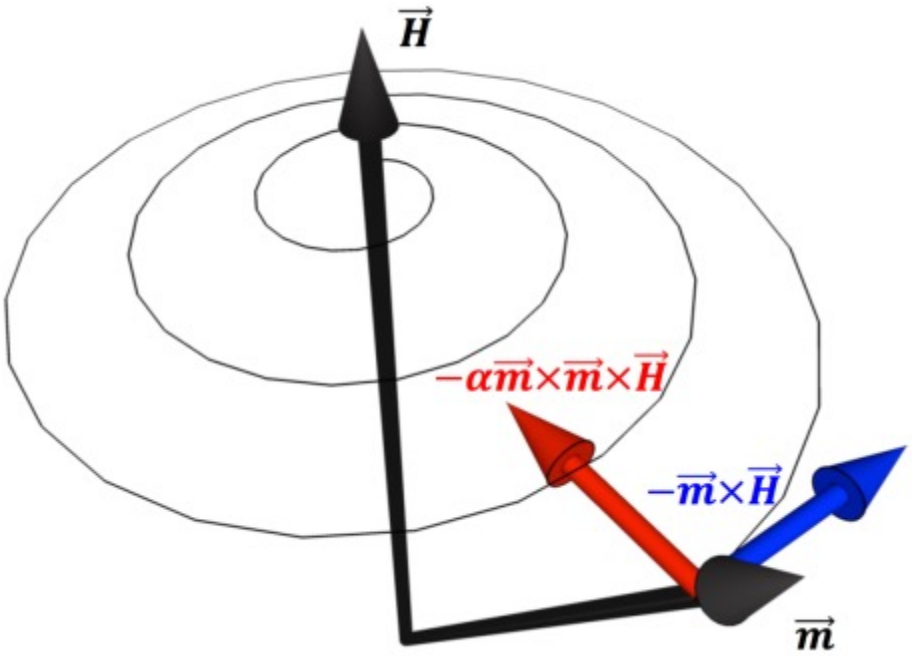

Due to losses with the surrounding medium, the magnetization vector follows the path of a decaying spiral as it undergoes dynamic precession. (Larmor + damping)

Superparamagnetism

- Small magnetic particles have moments that fluctuate their orientation due to thermal excitations as seen in the previous slide.
- For single particles above a certain temperature (the "blocking" temperature) the net magnetization over an extended time is zero. This is given by the Neel relation:

$$\tau = \tau_0 e^{KV/k_B T}$$

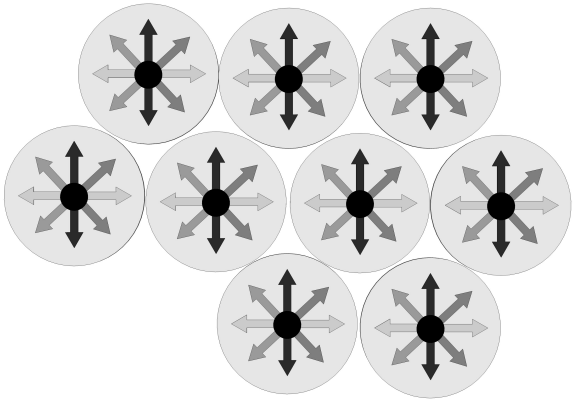

- Where τ_0 is the attempt time (~1ns), K is the anisotropy constant, V is the particle volume and $k_B T$ is the thermal energy of the particle.
- The magnetization is thus a nonlinear function of the external magnetic field.
- This effect causes the M-H curve of the particles to close, exhibiting no remanence or coercivity.

The Kittel Equation for Spheres

We recall the Kittel equation determines the resonant frequency of ferromagnetic structures and is given by:

$$f_0^2 = \mu_0^2 \gamma^2 [H_0' + (\mathcal{N}_x - \mathcal{N}_z)M]\left[H_0' + \left(\mathcal{N}_y - \mathcal{N}_z\right)M\right]$$

Where $\gamma \approx 28GHz/T$ is the gyromagnetic ratio, $\mathcal{N}_i$ is the demagnetizing factor along the i^{th} axis, H_0' is the effective field and M is the magnetization.

For spheres $\mathcal{N}_x$= $\mathcal{N}_y$= $\mathcal{N}_z$=1/3 and the resonance reduces to

$$f_0 = \mu_0 \gamma H_0' = \gamma B_0'$$

Thus for an ideal isolated sphere the resonant frequency is linear in the applied field.

UNIVERSITY OF SOUTH CAROLINA

Coplanar Waveguide (CPW)

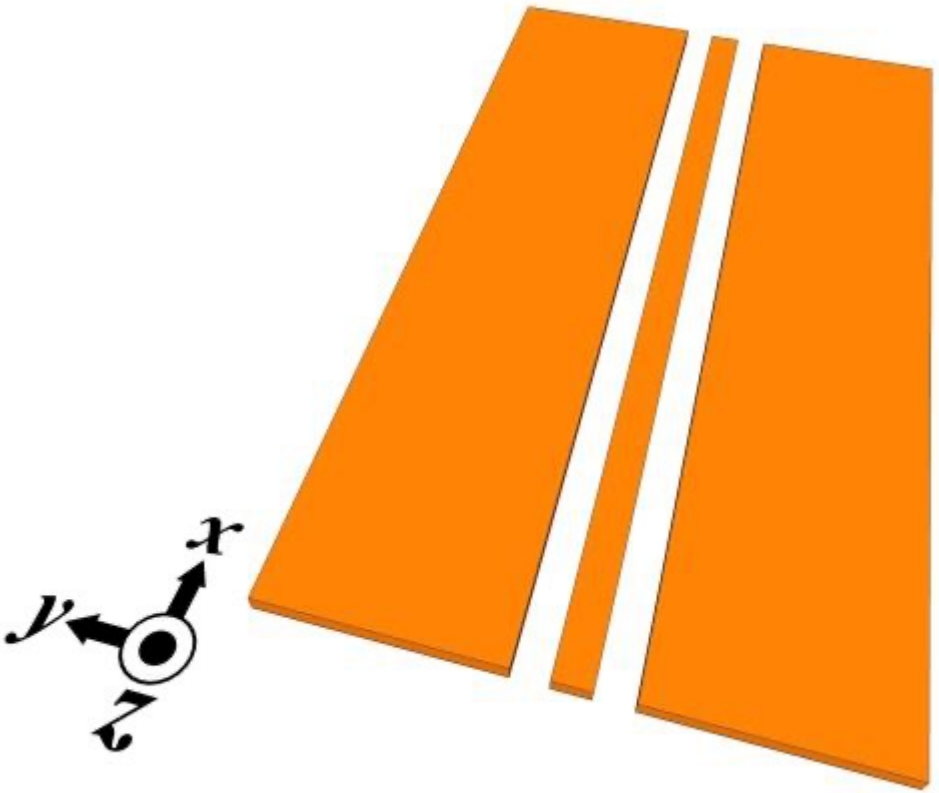

The inductive technique requires a coplanar waveguide (CPW). A general topology is shown on left.

Typically a magnetic sample is placed directly on the center of the waveguide. To use this technique with a liquid, a modified approach will be required to contain the sample.

UNIVERSITY OF SOUTH CAROLINA

Waveguide Channel

A channel is created with Bondic epoxy that cures instantly under UV light. Containing the fluid and preventing movement and evaporation are critical to the success of the measurements.

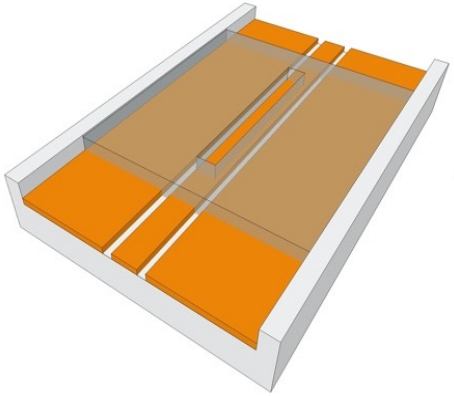

Step 1:

Initially a 1cm long, 0.75mm wide strip of tape is placed along the center trace as a mask using a stereoscope and the liquid epoxy is applied.

The tape is pulled up as the UV light is used to cure the liquid into a solid channel, leaving the copper trace exposed, but covering the gaps between ground.

UNIVERSITY OF SOUTH CAROLINA

Waveguide Channel

A channel is created with Bondic epoxy that cures instantly under UV light.

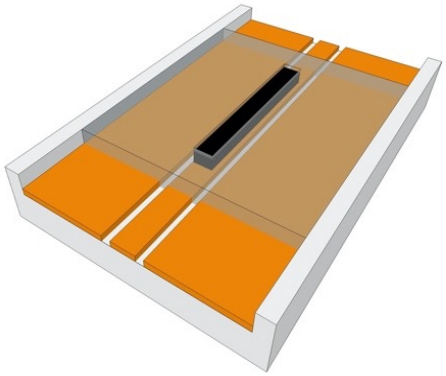

Step 2:

Undiluted ferrofluid is placed into the solid channel with a small pipette being careful not to overfill it.

UNIVERSITY OF SOUTH CAROLINA

Waveguide Channel

A channel is created with Bondic epoxy that cures instantly under UV light.

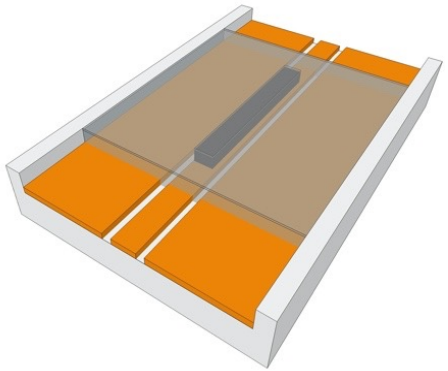

Step 3:

The ferrofluid is then surrounded by more liquid epoxy and it is allowed to slowly cover the sample as it is cured in stages if necessary.

If done carefully the epoxy floats on the denser ferrofluid long enough to be cured and forms a complete encasement.

UNIVERSITY OF SOUTH CAROLINA

Waveguide Channel

A channel is created with Bondic epoxy that cures instantly under UV light.

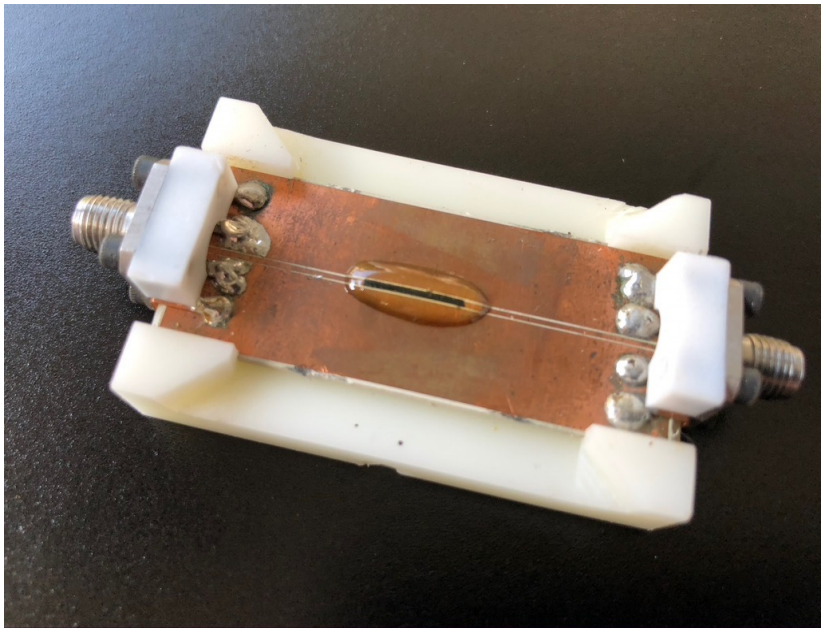

The finished channel encasing the ferrofluid strip directly above and in contact with the center trace.

Note the ferrofluid is not over the gap between signal and ground. This is critical to signal integrity.

The epoxy has no magnetic qualities and lifts off easily from the waveguide with no damage as it is not actually adhesive. Ferrofluid was found still liquid even after one week.

UNIVERSITY OF SOUTH CAROLINA

Inductive Technique Overview

Coplanar waveguide With ferrofluid sample

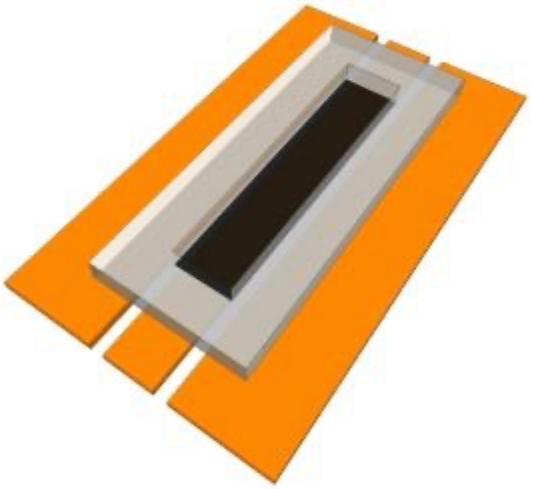

Current pulse gives a rapid *H* field reorientation

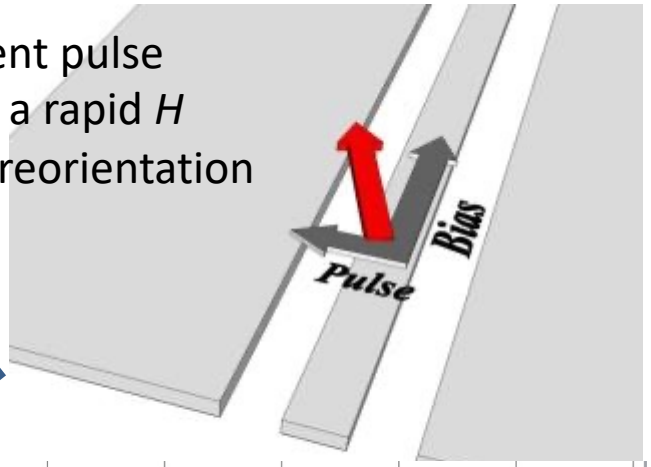

Time-changing magnetic field from particles

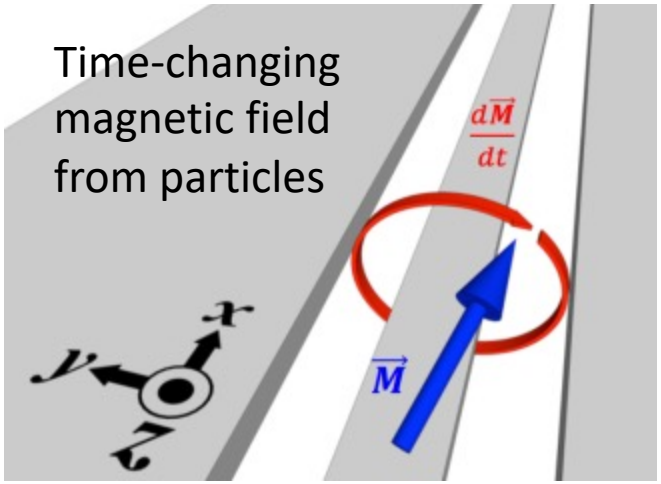

Induced voltage by Faraday's Law

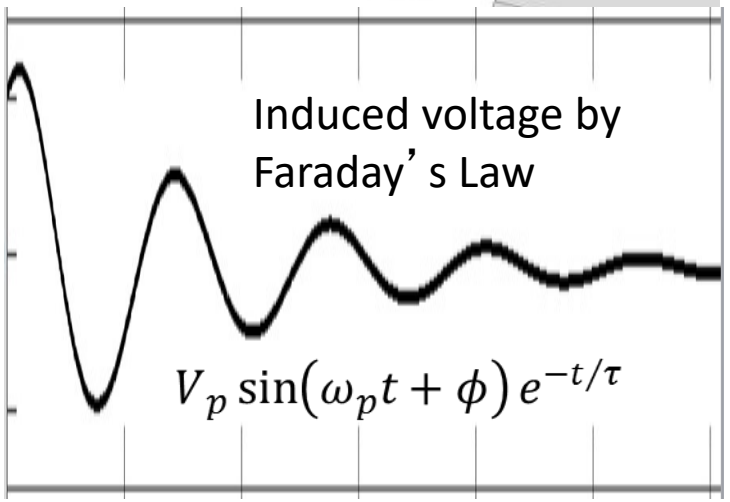

UNIVERSITY OF SOUTH CAROLINA

Experimental Layout

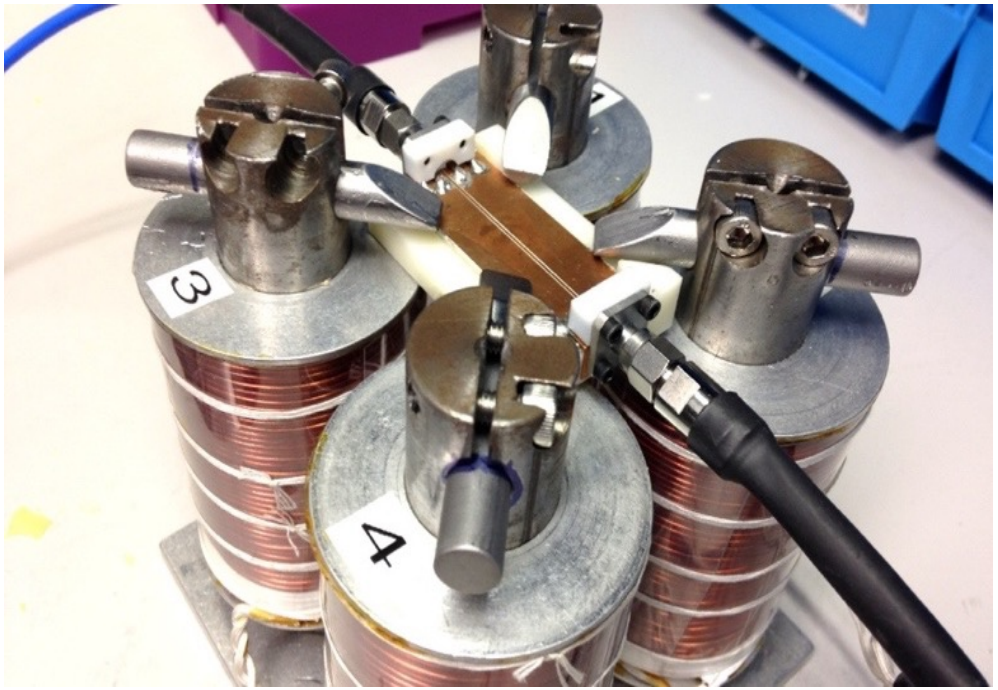

The CPW is placed inside a quadrupole magnet to provide a variable longitudinal magnetic field. This will also allow for a transverse saturation field in the zeroing step of the inductive technique.

UNIVERSITY OF SOUTH CAROLINA

Experimental Block Diagram

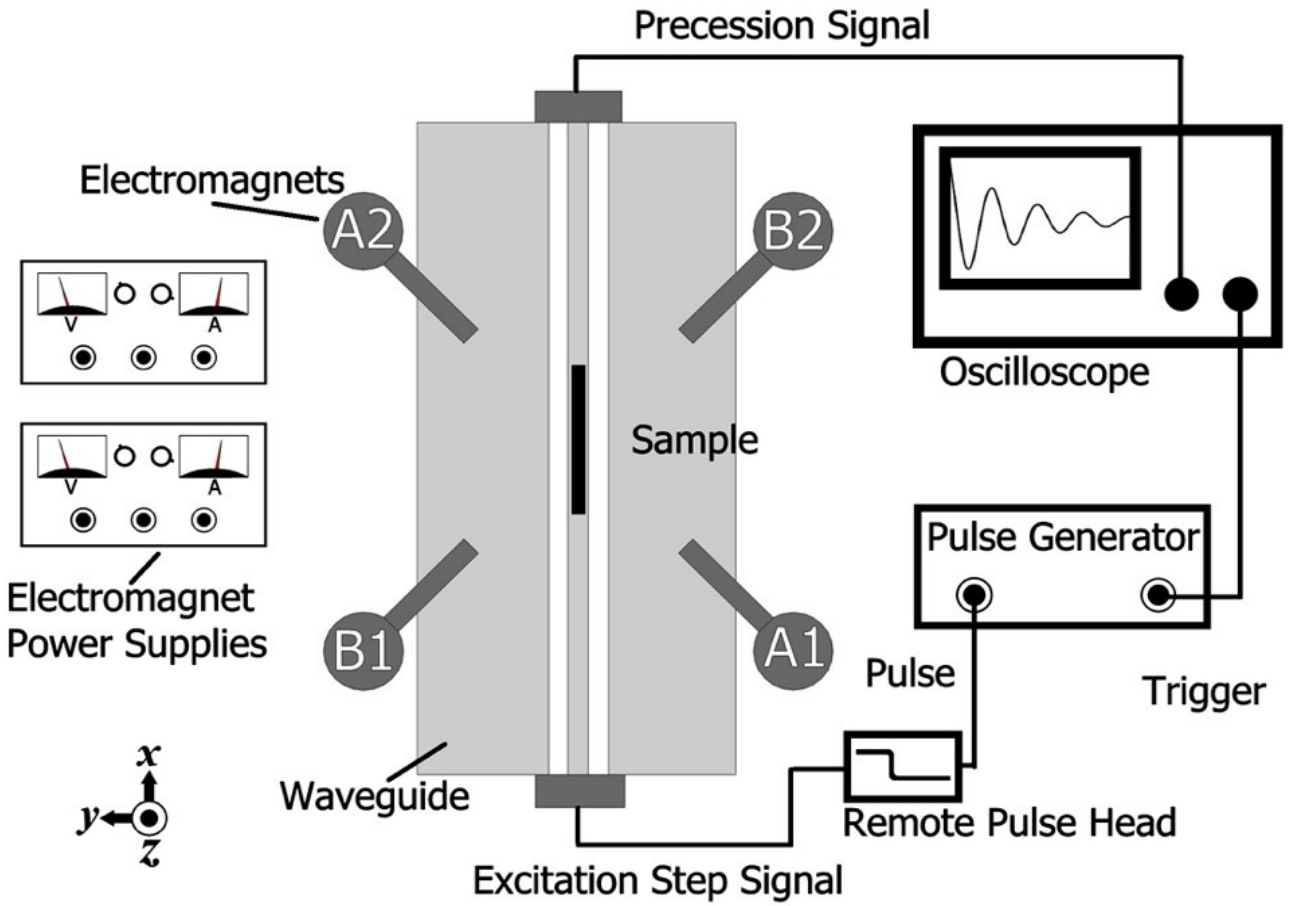

UNIVERSITY OF SOUTH CAROLINA

Measured Data: First 6 Bias Fields

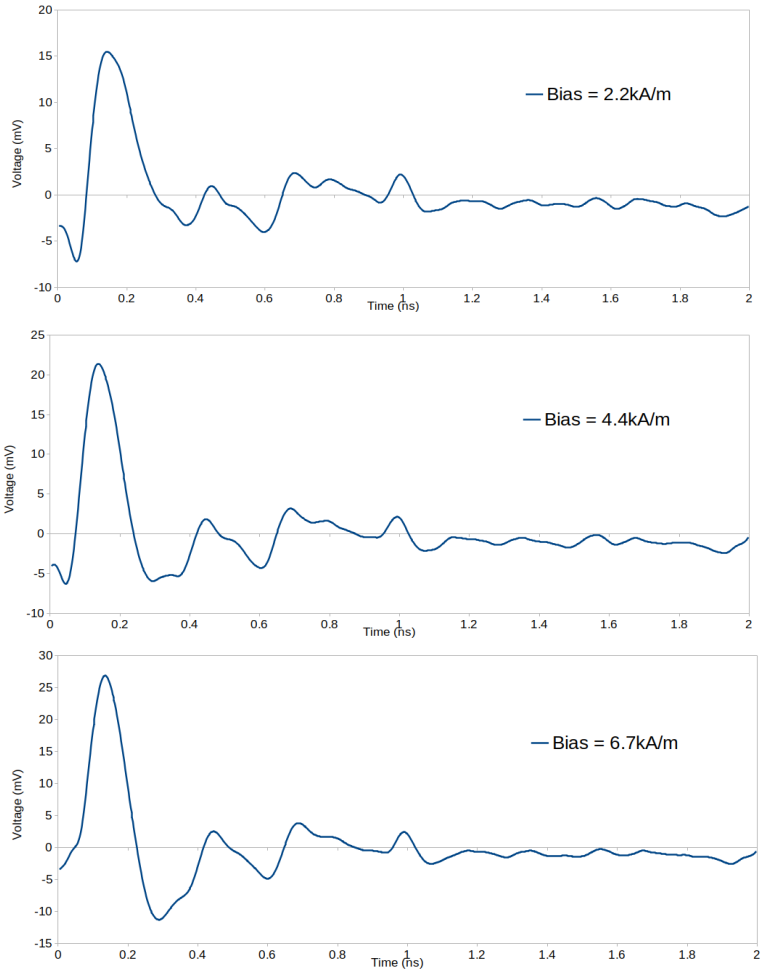

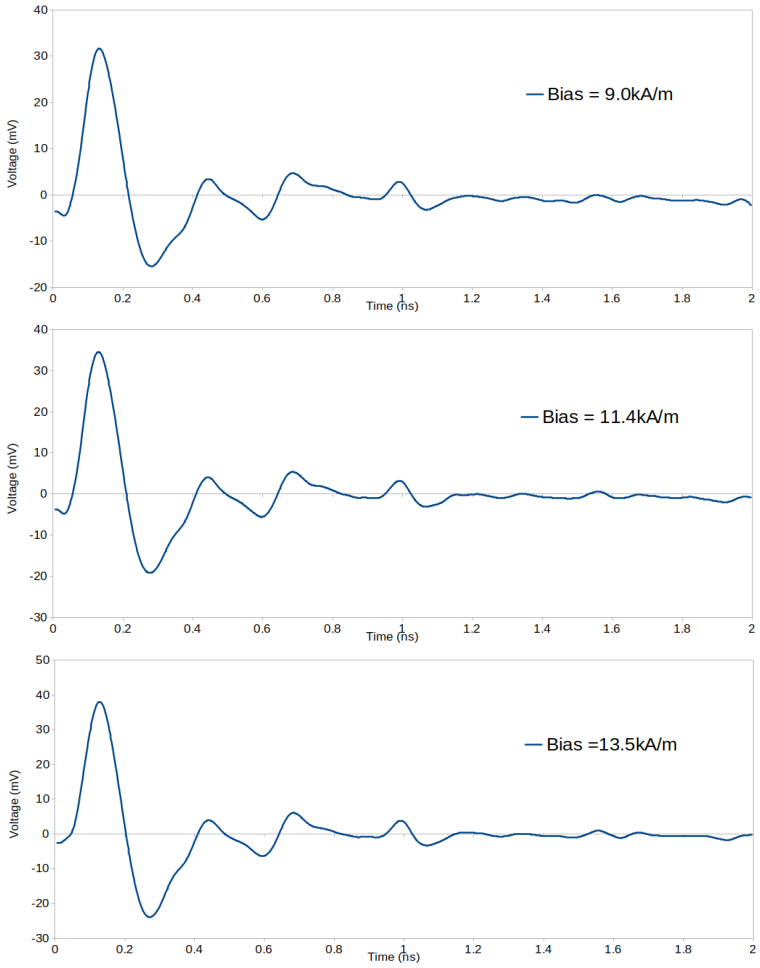

UNIVERSITY OF SOUTH CAROLINA

Measured Data: Last 6 Bias Fields

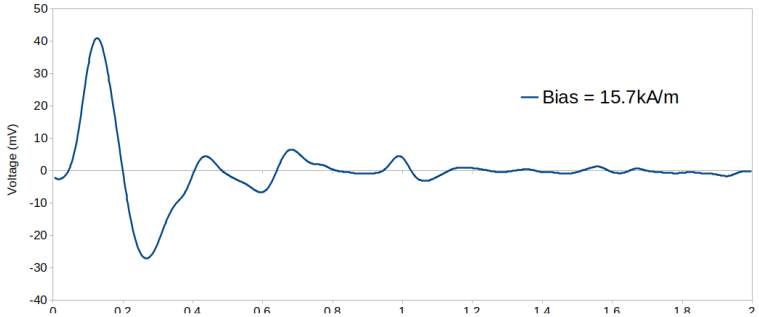

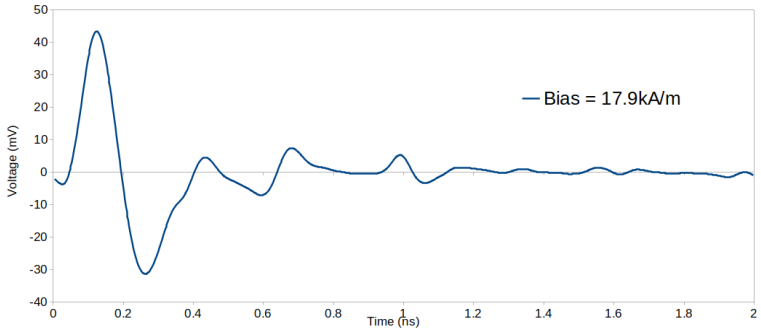

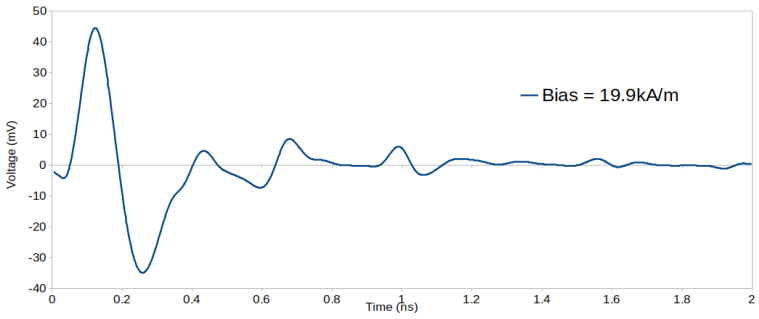

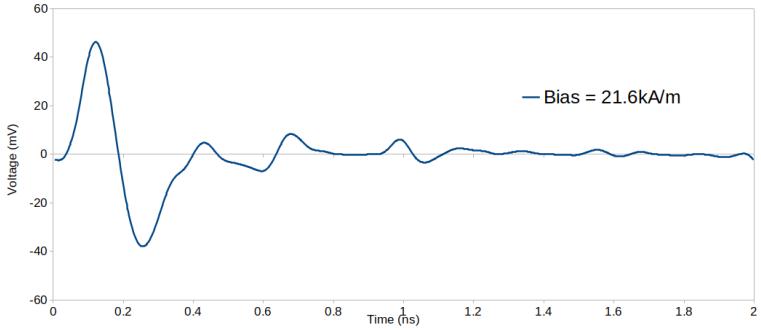

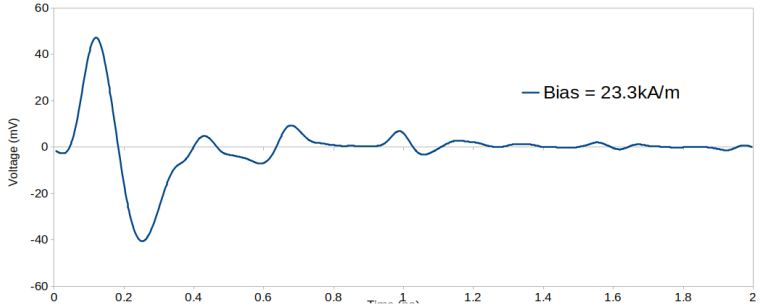

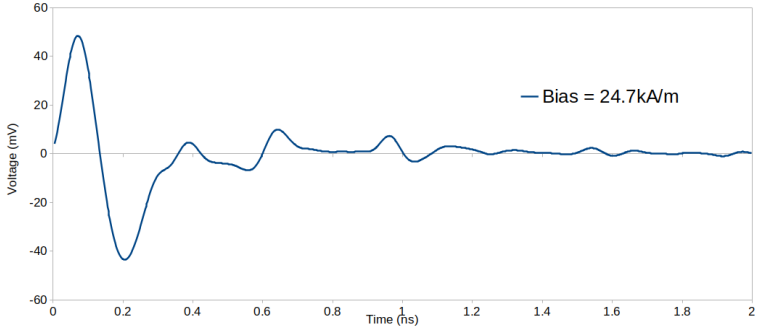

UNIVERSITY OF SOUTH CAROLINA

Measured Data: First and Last Signals

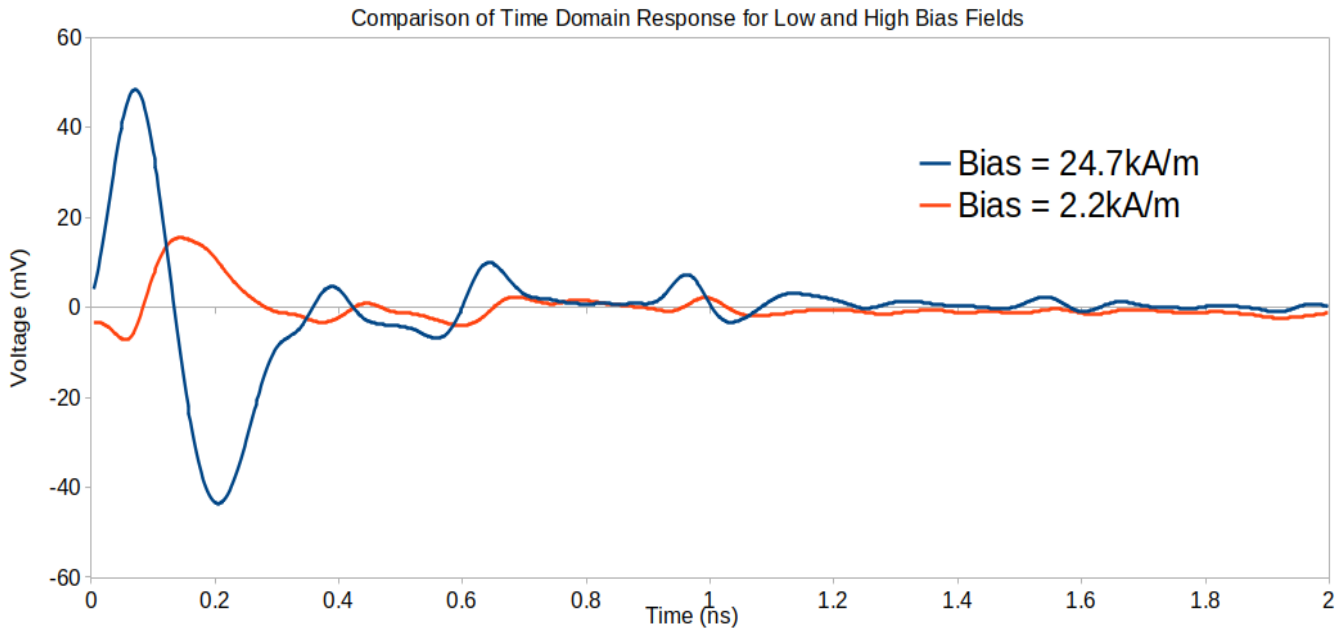

The first and last signals for relative comparison. This plot and the preceding two slides used a **smoothed** data set for initial impressions. In what follows and in all analyses, the **raw** data are used.

UNIVERSITY OF SOUTH CAROLINA

FFTs of Various Bias Fields

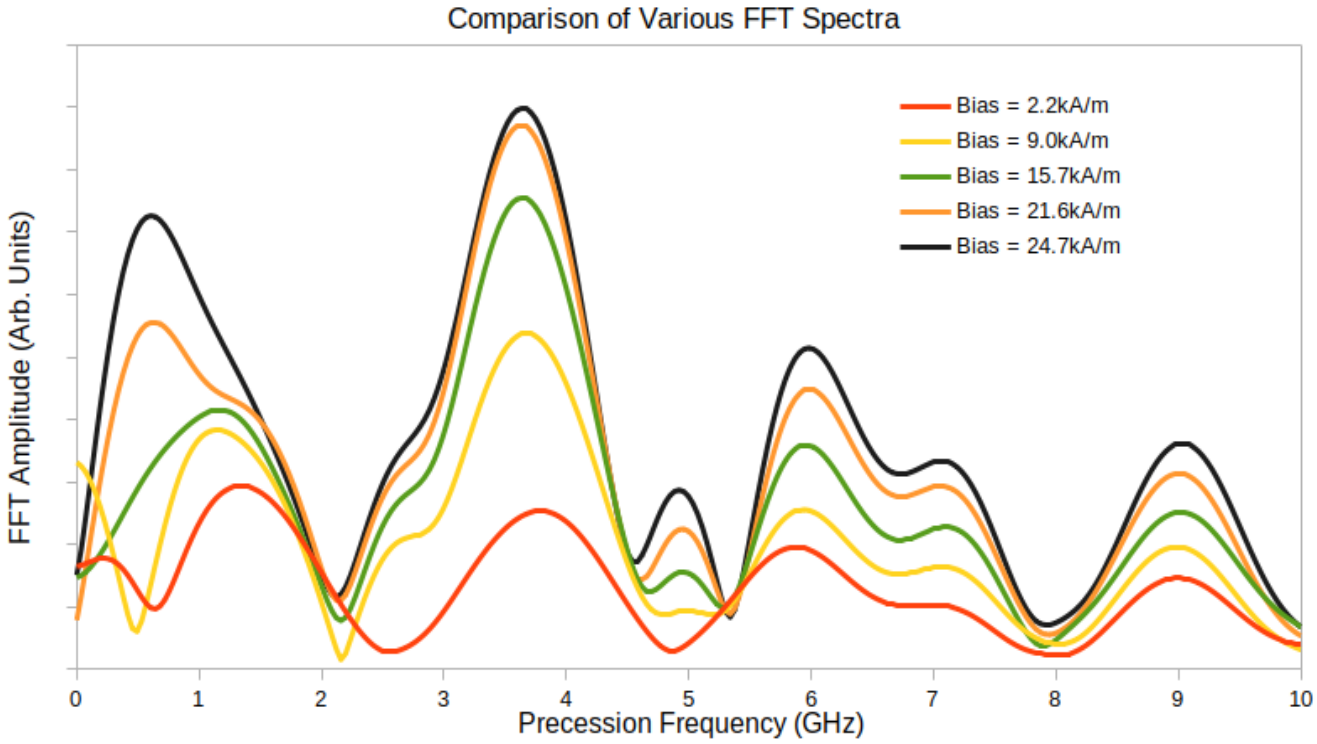

Some FFT spectra of various signals. Frequency response is relatively flat after 10GHz. Each spectral peak was found from time-domain model which will be discussed next.

UNIVERSITY OF SOUTH CAROLINA

FDTD Time-Domain Computer Model: Vinamax

- Vinamax is a FDTD algorithm written by J. Leliaert. It solves the Landau-Lifshitz equation using a macrospin approximation and was designed expressly for nanoparticle research.
- It is free software that runs in a Linux environment and requires the user to code their "world" of nanoparticles to be simulated. It is written in the computer language Go.
- The user codes the conditions and parameters and calls the solver from the command line prompt.
- Typical parameters include applied fields, particle position coordinates, anisotropy constant, magnetic and hydrodynamic radii, saturation magnetization, damping constant, time step and more.
- The exact waveform from my step signal was converted into magnetic field units and imported into the code. Thus the experiment was modeled with realistic conditions.

FDTD Time-Domain Computer Model: Particle Interaction

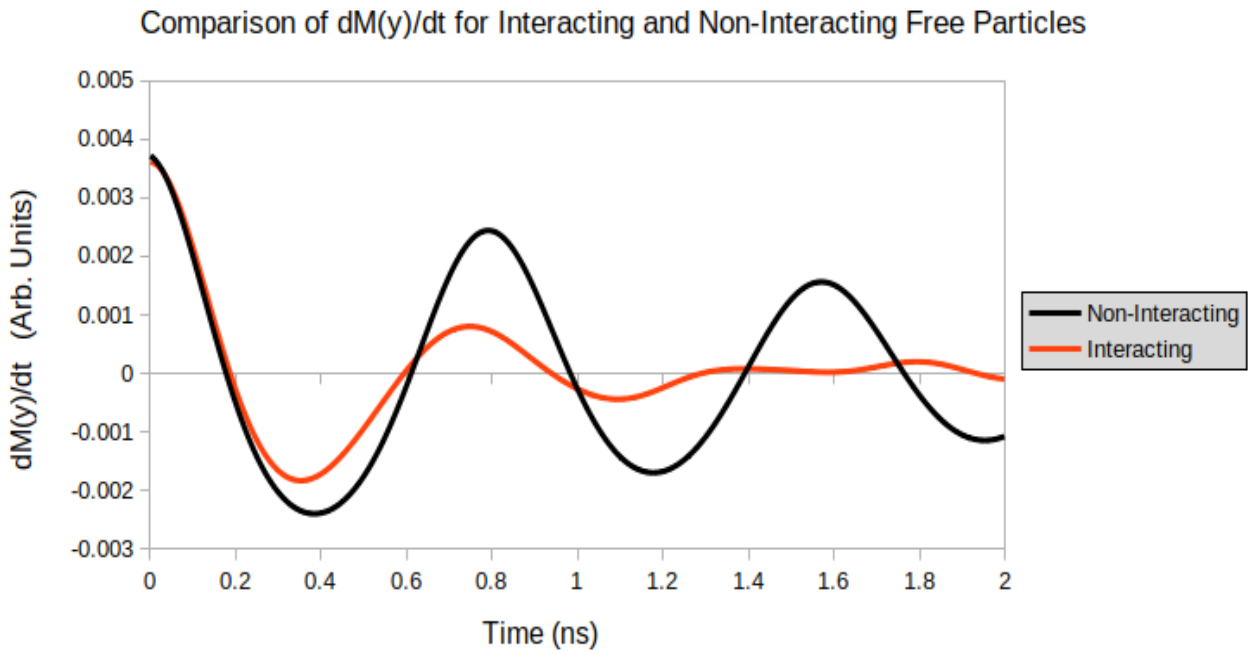

Compared plots of the derivative of interacting and noninteracting free particles in the time domain under otherwise identical parameters. It is seen the damping is affected by interactions.

UNIVERSITY OF SOUTH CAROLINA

Chain Dynamics

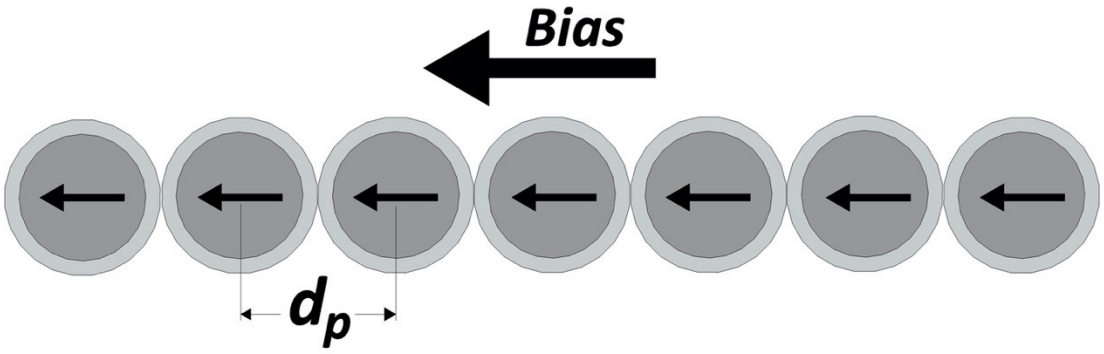

- It is well known from the literature that particles in ferrofluids can form chains.
- The average length and number of chains has been shown to increase under external fields
- This formation is a low energy state for magnetized particles and naturally increases the effective field of each neighbor. The dipolar field of a particle is given by:

$$\vec{\boldsymbol{B}} = \frac{\mu_0}{4\pi r^3}\left[3(\vec{\mathfrak{m}} \cdot \hat{\boldsymbol{r}})\hat{\boldsymbol{r}} - \vec{\mathfrak{m}}\right]$$

UNIVERSITY OF SOUTH CAROLINA

Chain Dynamics

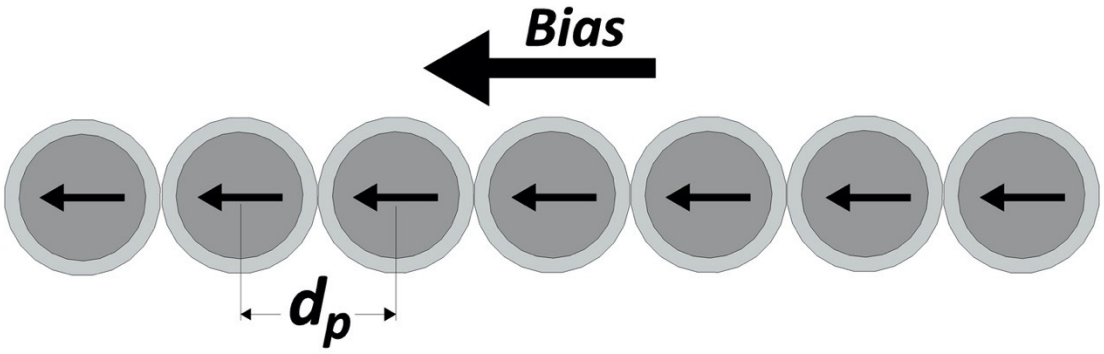

- For *N* identical particles in a straight chain it was derived for this analysis that the effective field for particles near the center is

$$\vec{B}_{dip} = \frac{\mu_0 |\vec{\mathfrak{m}}|}{\pi} \sum_{i=1}^{N} \frac{1}{(i\ d_p)^3}$$

- Where $\vec{\mathfrak{m}}$ is the particle moment and d_p is the interparticle distance.
- This means that as the chain length gets large the effect of each additional particle has a diminishing effect on particles near the center (or far away in the chain).
- Thus the expected resonant frequency of a chain saturates.

Chain Dynamics: Saturation of Effective Field

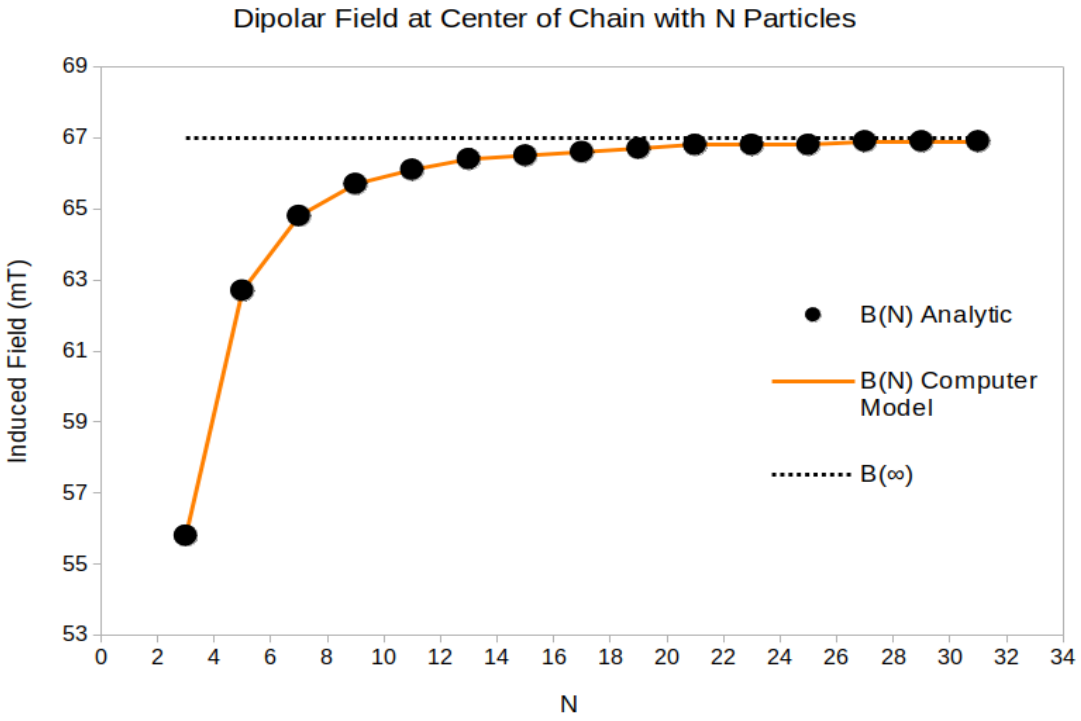

Points from the foregoing equation plotted against a Matlab script that solves the dipole equation explicitly for chains. For the $10nm$ particles under consideration the max field contribution is $B_{max} \approx 67mT$.

UNIVERSITY OF SOUTH CAROLINA

FDTD Time-Domain Computer Model: Chain Simulation

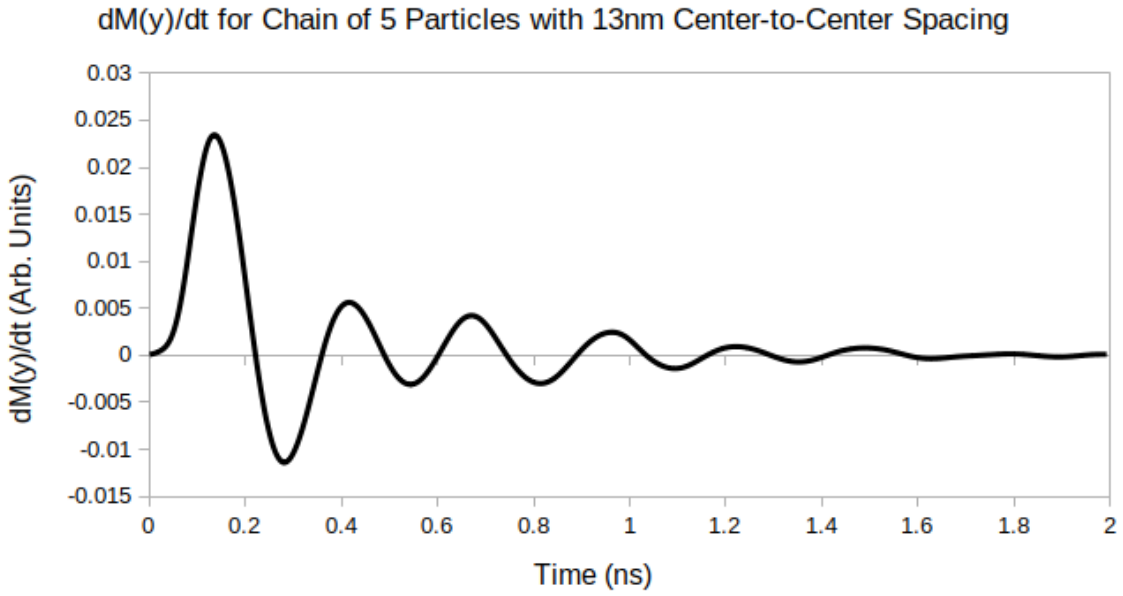

Derivative of the time-domain signal for a chain of 5 particles where $d = 13nm$. Note this indicates a coating of $1.5nm$ assuming the particle coatings are in contact.

UNIVERSITY OF SOUTH CAROLINA

FDTD Time-Domain Computer Model: Particles and Chain Simulation

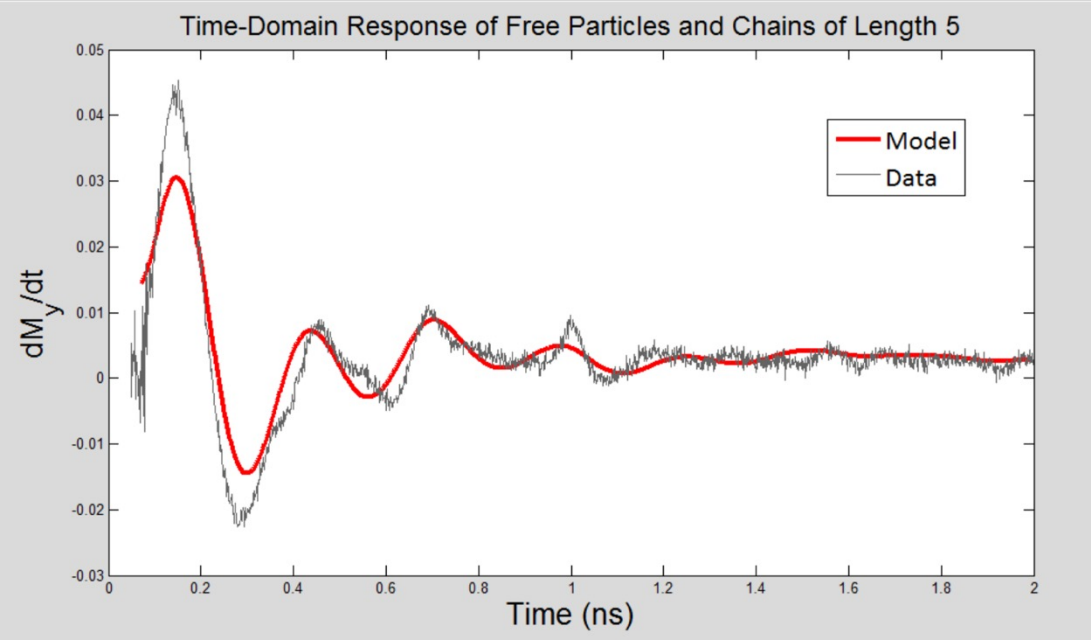

Result of free particles and chains of $N = 5$ with simulated values of $H_b = 13.5\frac{kA}{m}, M_s = 480\frac{kA}{m}, |K| = 12\frac{kJ}{m^3}$, $R = 5nm, d_p = 13nm,$ $\alpha = 0.12.$

UNIVERSITY OF SOUTH CAROLINA

FDTD Time-Domain Computer Model: Particles and Chain FFT

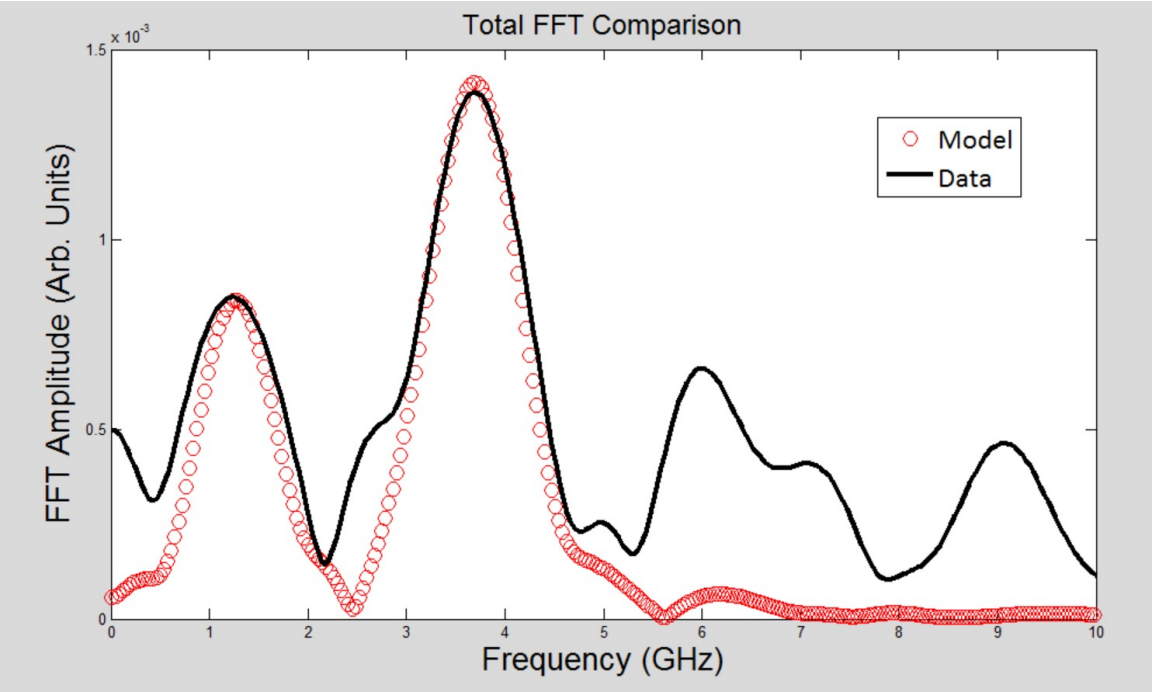

FFT of the foregoing time-domain model. Note the higher frequency is a result of the chains. Using the anisotropy of $|K| = 12\,\frac{kJ}{m^3}$ and the saturated chain field discussed previously, one expects $f = 3.76GHz$.

UNIVERSITY OF SOUTH CAROLINA

FDTD Time-Domain Computer Model: Higher Frequencies

- It is clear from looking at the FFT for collections of particles and chains that there is significantly higher frequency content missing from the signal around $6GHz$ and $9GHz$. There is also a smaller lobe around $7GHz$.
- Attempts to get the model to match these frequencies by interparticle interactions in various structures were unsuccessful.
- There is much published research and literature about higher anisotropy appearing in magnetic nanoparticle systems.
- Modifying the anisotropy constant to $K_{eff} = 53\,\frac{kJ}{m^3}$ in Vinamax with the particles and chain simulations, shifted the two peaks for those responses over to the $6GHz$ and $9GHz$ regime. This is larger by a factor of around 4.4.
- The complete data fits are presented next followed by an analysis.

UNIVERSITY OF SOUTH CAROLINA

Fitted Data: First 6 Bias Fields

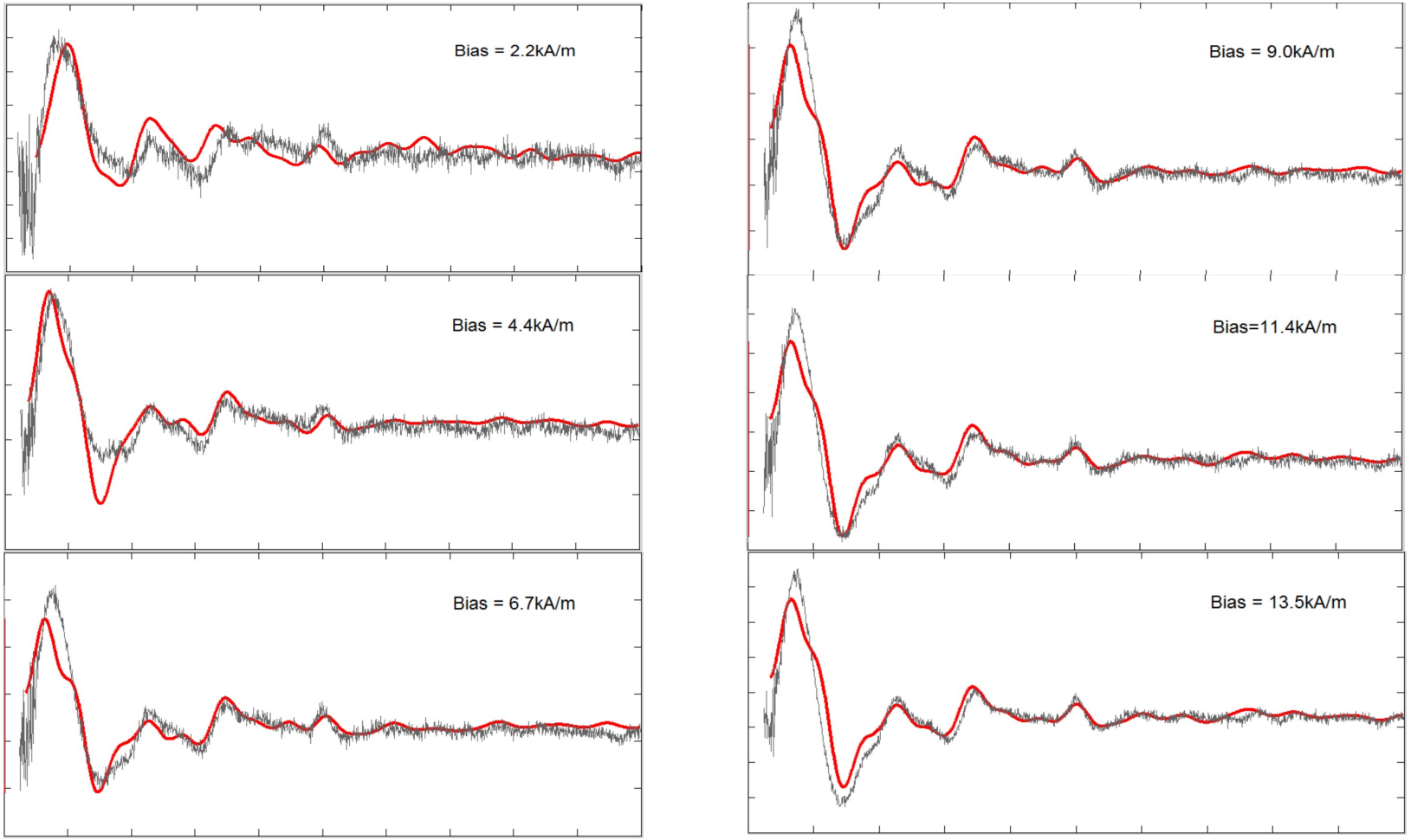

UNIVERSITY OF SOUTH CAROLINA

Fitted Data: Last 6 Bias Fields

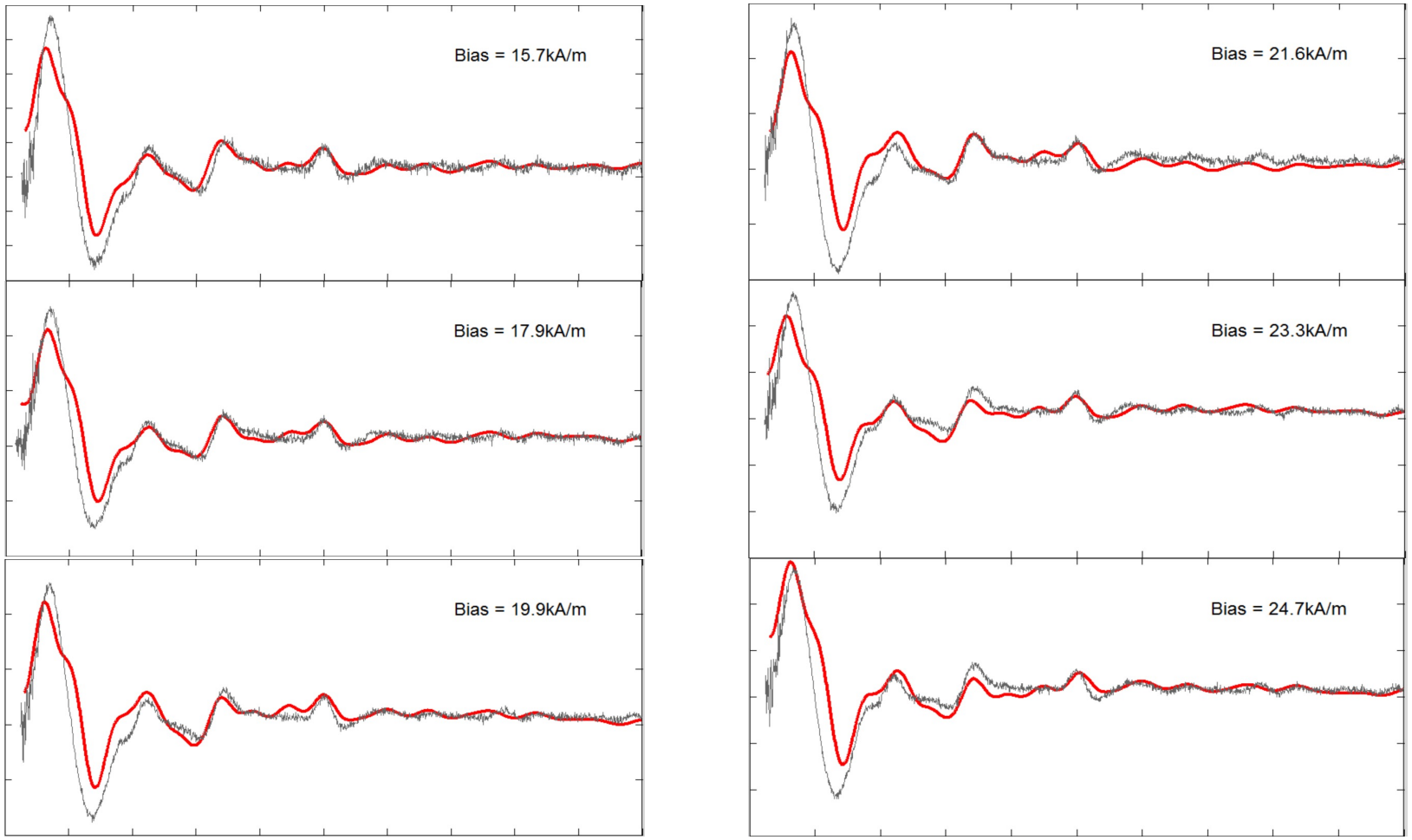

UNIVERSITY OF SOUTH CAROLINA

Fitted Data: Some FFT Example Fits

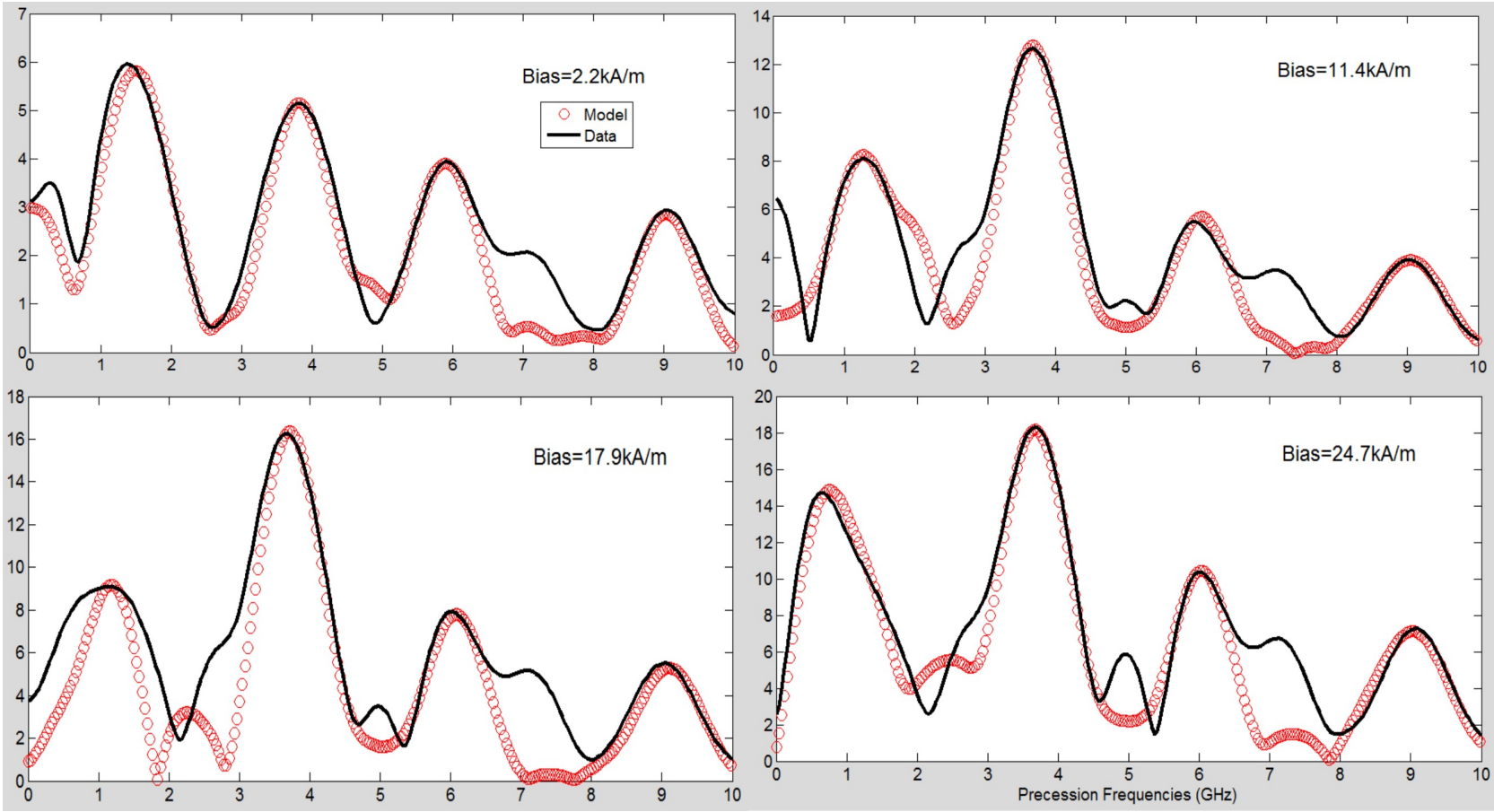

UNIVERSITY OF SOUTH CAROLINA

FDTD Time-Domain Computer Model: Quality of Fit

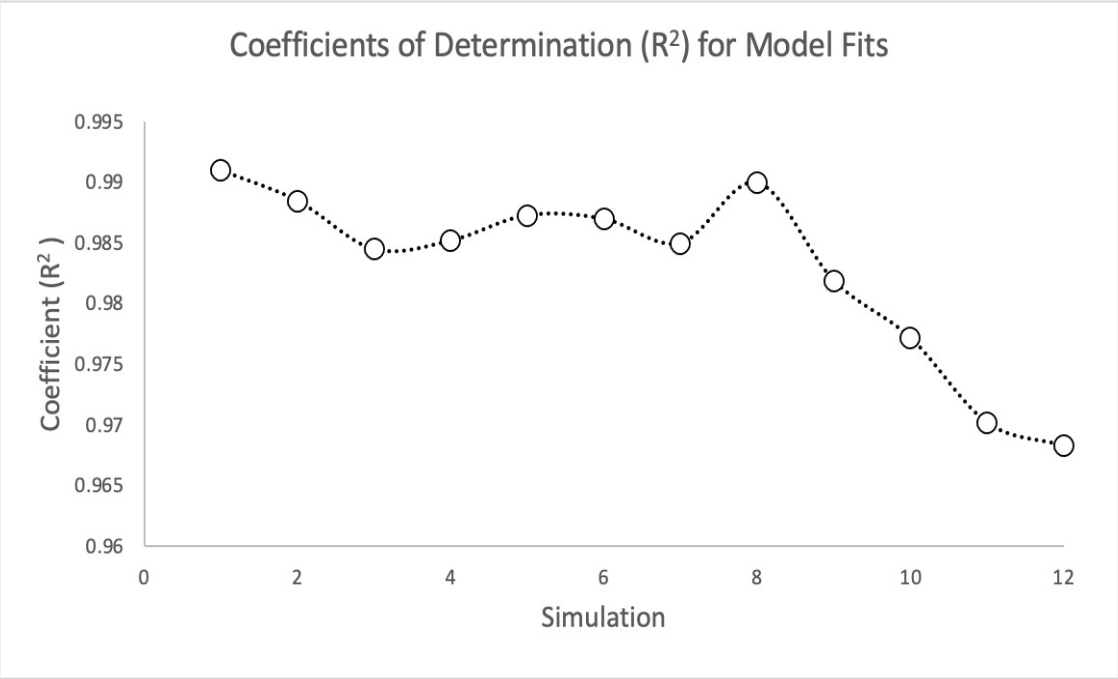

R^2 values of each time-domain fit.

UNIVERSITY OF SOUTH CAROLINA

FDTD Time-Domain Model Analysis

- Chains in this work all had a minimum of $N = 5$ particles. Smaller chains exhibited a side lobe around $2GHz$ not present in the data (this is caused by end behavior dominating the response).
- The resonant frequencies of chains were seen to actually *decrease* with increasing field. This was predicted by the model as the number of chains grew (chain density increasing). Lateral demagnetizing effects were apparent as more chains formed and were crowding closer to one another.

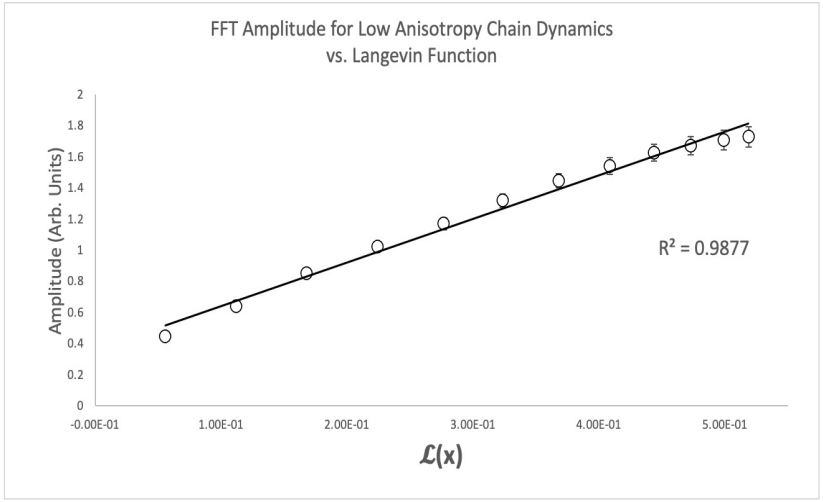

The FFT amplitude of the chains grows linearly with a Langevin function likely indicating more chain formation as the as particles transition from SPM regime to the blocked regime.

UNIVERSITY OF SOUTH CAROLINA

FDTD Time-Domain Model Analysis
Interchain Interactions

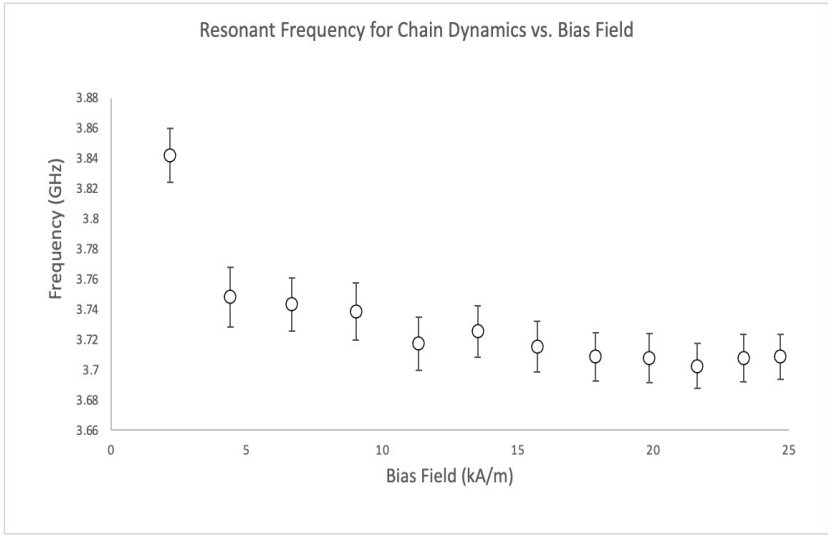

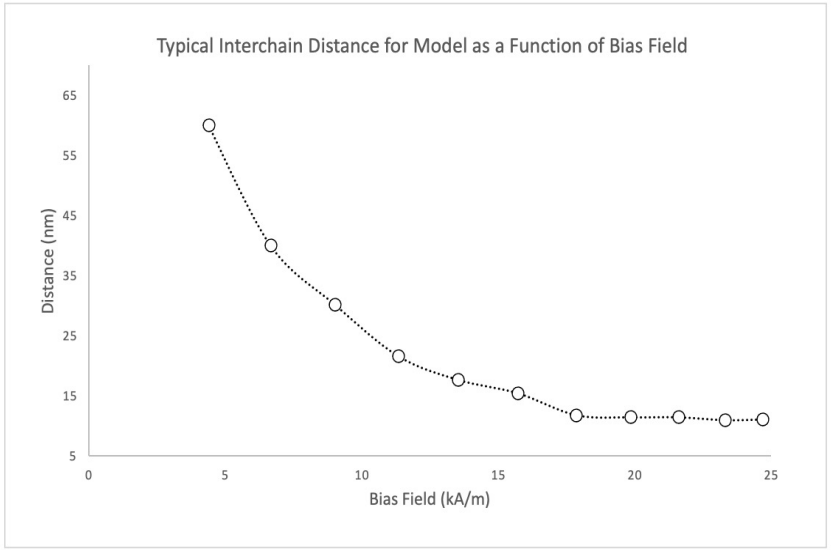

Frequencies of chain formations under increasing bias field (left). Model predicted this frequency decrease as nearest neighbor chains continued to form closer to one another. Average interchain distances shown on right. Note the asymptotic behavior at the end.

UNIVERSITY OF SOUTH CAROLINA

High Anisotropy Analysis

- While the increased anisotropy was able to make the fit work best, the decision to increase it was not arbitrary. There are many reports of such an increase in small particle systems.
- Often this increase is attributed to a spin disorder occurring at the particle surface where the crystal symmetry is broken. Smaller particles have a higher fraction of their atoms on the surface than larger ones.
- This reasoning was first made by Neel in the late 1940s.
- The following expression has been found used to relate the surface energy density term, K_s to the bulk value as an effective energy density:

$$K_{eff} = K_{\infty} + \frac{6K_s}{D}$$

Where K_{∞} is the bulk value and *D* is the particle diameter.

- Using the fitted value of $K_{eff} = 53 \frac{kJ}{m^3}$ there is still a decision left as to which diameter should be used before solving for K_s.

UNIVERSITY OF SOUTH CAROLINA

High Anisotropy Analysis

- Many reports of commercial ferrofluids (including the present manufacturer) have shown the particle diameters to be distributions around a mean, $10nm$ in this case.
- Many reports show this increase in anisotropy occurs for diameters smaller than $5nm$ and some report no effect until $3nm$.
- It was found that modeling particles with $D = 3nm$ made the error in the time-domain fit minimal as well as the FFT alignment. This gives $K_s = 2.05\times10^{-5}\,\frac{J}{m^2}$.
- This value is within the range reported by several authors found by different methods so it is tentatively assigned to the cause of the increase in effective anisotropy.
- It should be noted this technique lacks the spatial resolution necessary to determine the actual cause, but the data and model along with the agreement of the fitted parameter permit cautious speculation.

UNIVERSITY OF SOUTH CAROLINA

High Anisotropy Particle Analysis

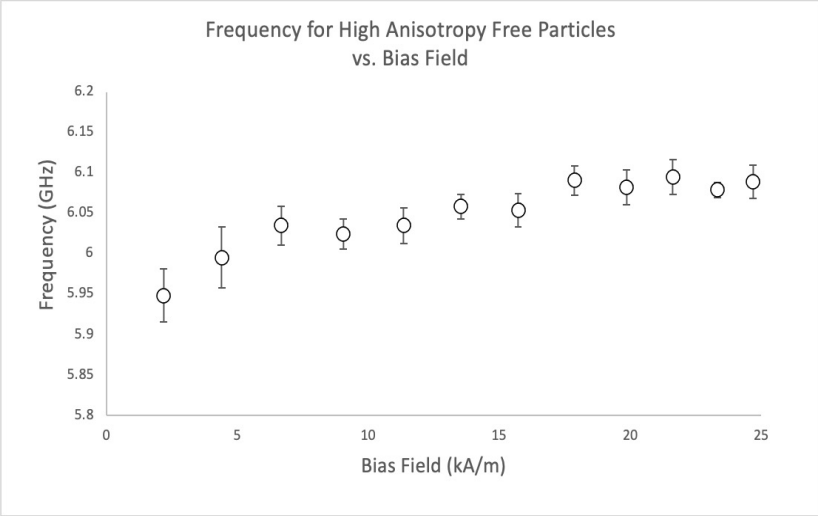

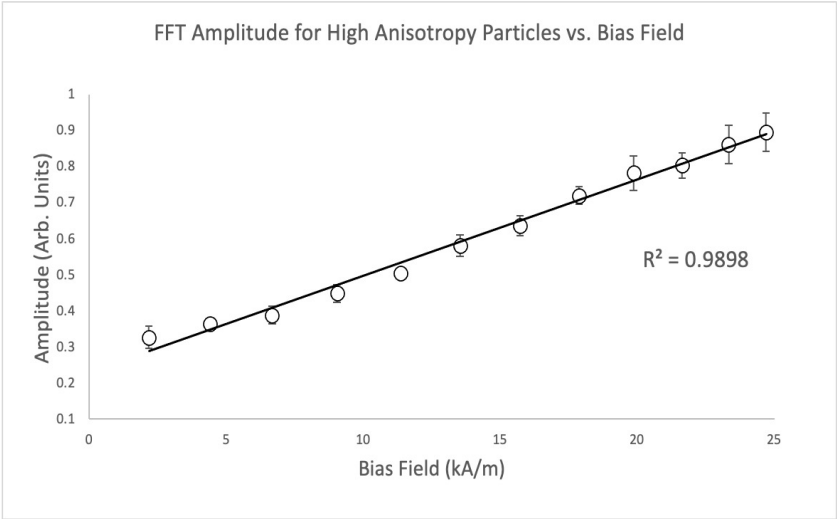

The $6GHz$ frequencies as a function of bias field (left). The frequencies generally increase with bias field, but it is not monotonic. Sample rearrangements occur to minimize the energy of collections as the field changes which cause can demagnetization.
FFT amplitude is linear in applied field (right).

UNIVERSITY OF SOUTH CAROLINA

High Anisotropy Chain Analysis

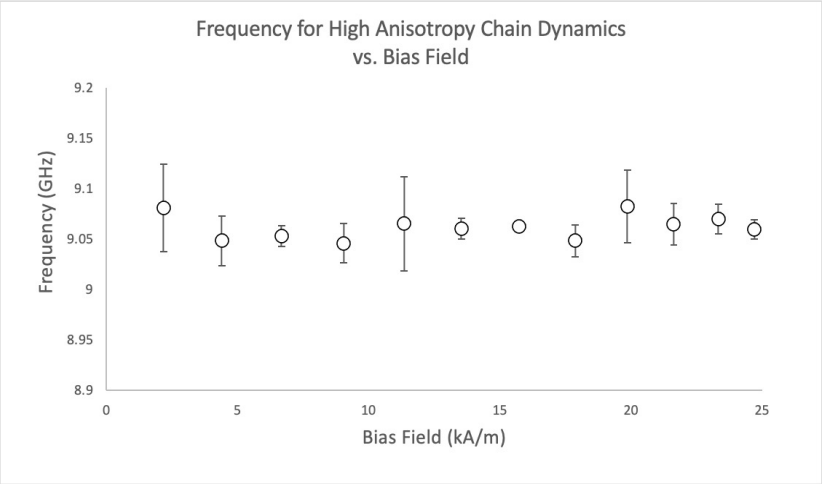

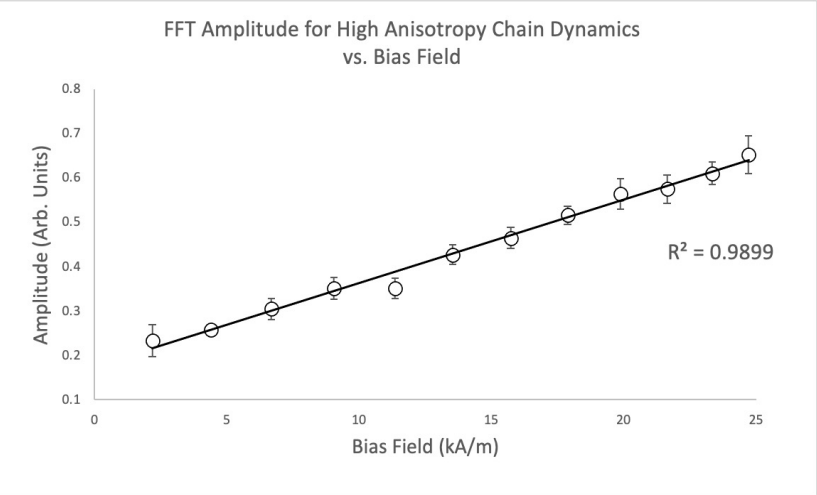

The $9GHz$ frequencies as a function of bias field (left). The frequencies were modeled with small particles in a chain structure. The frequency trend is similar to the normal chains but the initial dramatic decrease is not as evident. FFT amplitude is linear in applied field (right). The $7GHz$ lobe in the FFTs is a result of particles at the end of these chains. Efforts to make the amplitude of the $7GHz$ component match caused the time-domain fit to suffer.

UNIVERSITY OF SOUTH CAROLINA

Low Frequency Shift Analysis

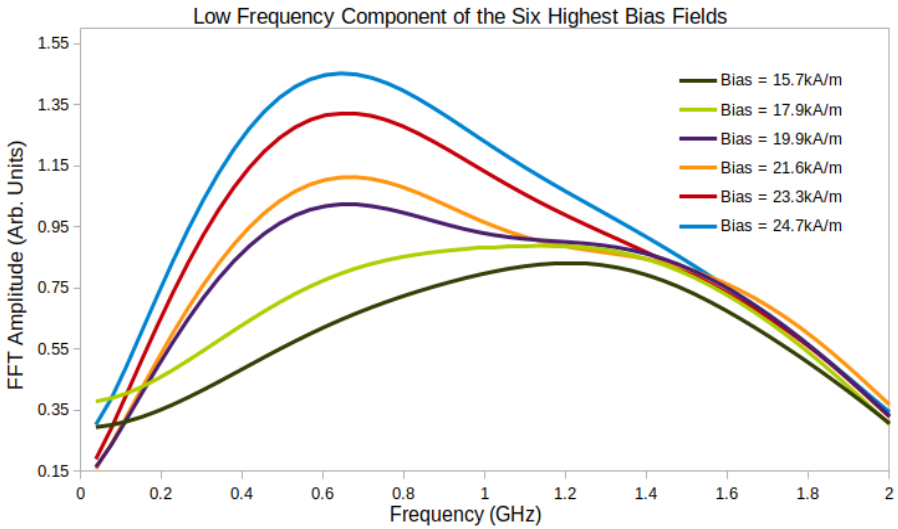

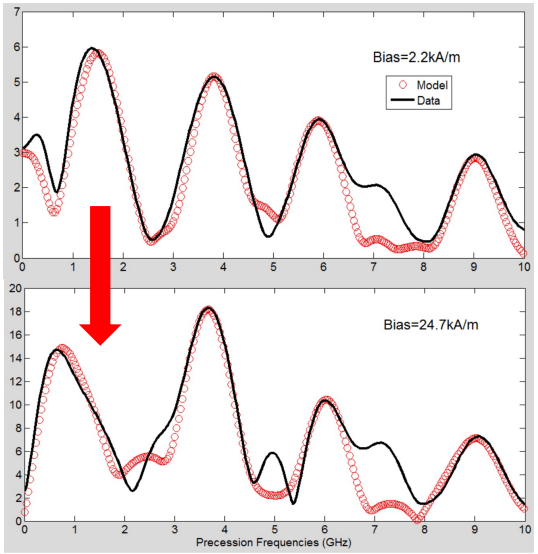

Bias fields above $H_b = 18\frac{kA}{m}$ cause a noticeable leftward shift in the lowest FFT component. This frequency peak is due to free particles and the shift is caused again by chains. As the chains begin to populate the sample volume, they demagnetize particles as well as one another. This was borne out by the model; the FFT can be seen to also shift shape in the model on the right. This phenomenon makes tracking lower resonant frequencies as a function of applied field difficult.

UNIVERSITY OF SOUTH CAROLINA

Magnetization Analysis

- It should be remembered that the inductive technique measures the ***derivative*** of the magnetization response.
- Since the signals are sinusoidal, magnetization components that that have high frequencies have amplitudes that are scaled by that frequency because of the derivative.
- To know what fraction of the sample is participating in a given resonance, one cannot simply look at the FFT amplitudes from measured data of that frequency.
- What is required is the FFT of the ***magnetization itself***, which is not directly observable with the inductive technique.
- Fortunately, the FDTD model provides the magnetization, requiring the user to take the derivative should they want it.

Magnetization Analysis
Estimating Population Reactions

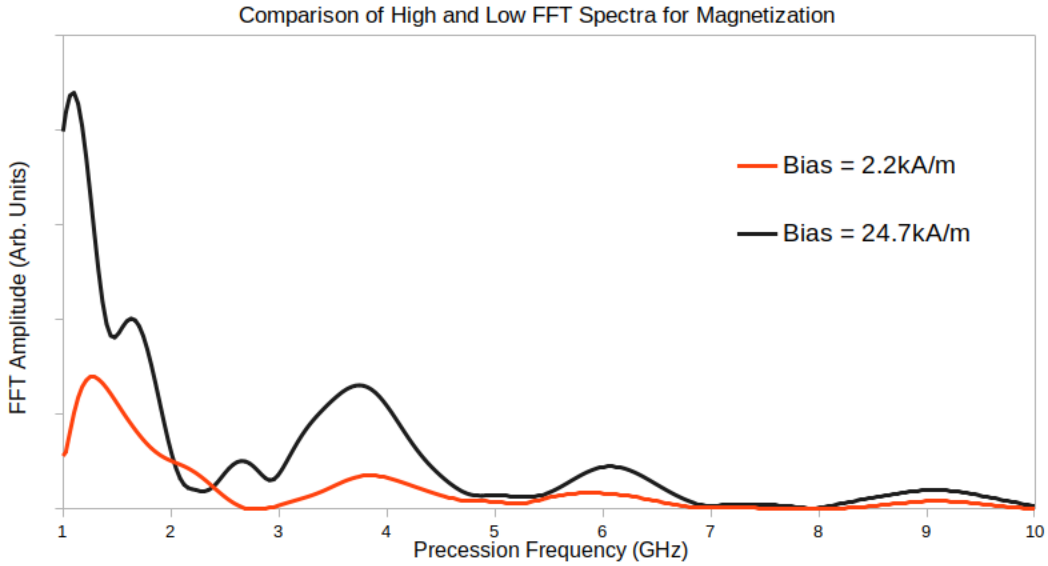

Derivative of the magnetization itself under max and min bias fields. Note the magnetization has a non-zero resting angle so there is a large DC offset. This part of the plot is removed to avoid dwarfing the relevant data. It is seen the high frequency components are quite small compared to lower frequencies.

UNIVERSITY OF SOUTH CAROLINA

Magnetization Analysis

Estimating Population Reactions

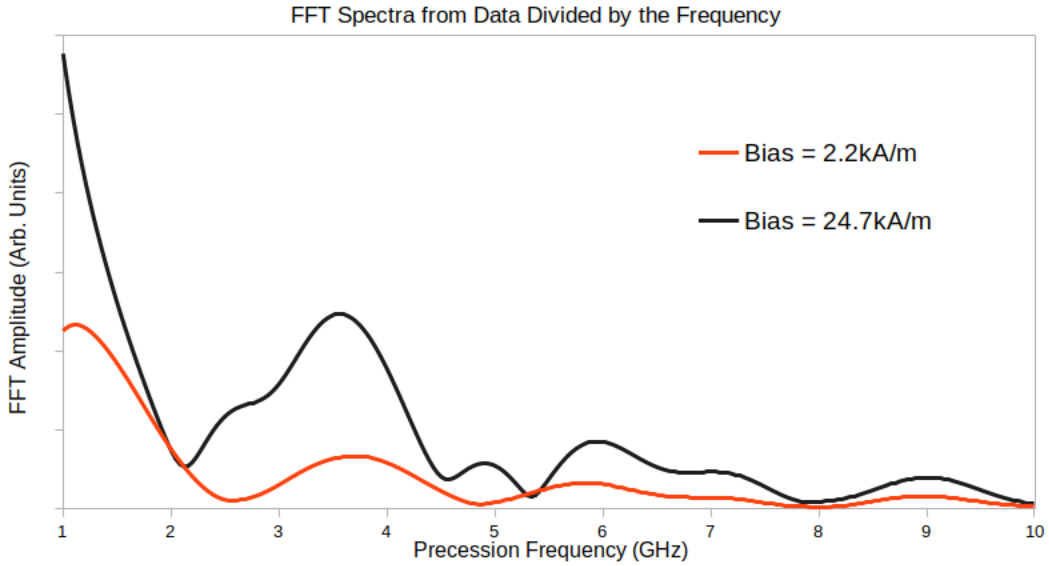

To estimate the relevant quantities with only the time-domain data (i.e., without using the model) the FFT was divided at each point by its frequency at that bin. This undoes the scaling imposed by the derivative. It does not account for the fact that the derivative of a damped sine wave is more complicated than scaling by the frequency.

UNIVERSITY OF SOUTH CAROLINA

Conclusions

- Time-domain measurements on ferrofluid using the inductive technique proved successful provided the sample is encased entirely.
- The FFT spectrum is very complicated.
- Using a FDTD macrospin solver (like Vinamax) one can model the data with fairly high fidelity if the sample geometry can be recreated in the model setup.
- This allows determination of which frequency peaks are caused by which type of phenomena.
- Normalizing the FFT amplitudes to their frequency bins can estimate the quantity of the sample that is responsible for a given resonance.
- The present sample was found to be mostly free particles with chain formation growing in a Langevin-type manner with bias field.
- The chains caused demagnetizing effects in other chains almost immediately and with free particles above $18kA/m$.
- The samples were found to return to their original state after the bias field was turned off.

UNIVERSITY OF SOUTH CAROLINA

Conclusions

- Evidence of high anisotropy in a small fraction of particles was observed.
- This was modeled as an effective anisotropy parameter value of $53kJ/m^3$. Adjusting the anisotropy parameter to this value caused the frequencies for particles and chains to shift to the $6GHz$ and $9GHz$ ranges, respectively.
- The cause of this effect is tentatively speculated to be due to surface effects widely reported in the literature.
- For $\mathrm{D} = 3nm$ particles the calculated value of the surface anisotropy term $K_s = 2.05\times10^{-5}\,\frac{J}{m^2}$ comports well with other findings, however the current technique cannot be used to independently confirm this hypothesis.

References

[1] Title Image: https://www.reddit.com/r/blender/comments/691xps/ferrofluid/

[2] J. M. D. Coey, *Magnetism and Magnetic Materials, Cambridge, Cambridge Press, 2010.*

[3] R. E. Rosensweig, *Ferrohydrodynamics, Mineola, Dover Publications, 2014.*

[4] C. P. Bean and J. D. Livingston, "Superparamagnetism," *J. Appl. Phys*. vol. 30, issue 4, S120, 1959.

[5] T.J. Silva *et al.*, "Inductive measurement of ultrafast magnetization dynamics in thin film Permalloy," *J. Appl. Phys*. vol. 85, no. 11, pp. 7849-7862 Jun. 1999.

[6] W. T. Coffey, P.C. Fannin, "Internal and Brownian mode-coupling effects in the theory of magnetic relaxation and ferromagnetic resonance of ferrofluids," *J. Phys.: Condens. Matter, vol. 14, pp. 3677-3692, 2002.*

[7] R. J. Deissler, *et al.,* "Dependence of Brownian and Neel relaxation times on magnetic field strength," *Med. Phys., vol. 41, no. 1, pp. 012301-1 – 012301-12.*

[8] W. F. Brown, Jr., "Thermal Fluctuations of a single-domain particle," *Phys. Rev. vol. 130, no. 5, pp. 1677-1686, Jun. 1963.*

UNIVERSITY OF SOUTH CAROLINA

References

[9] C. Kittel, “On the theory of ferromagnetic resonance absorption,” *Phys. Rev*. vol. 73, no. 2, pp. 155–161, Jan. 1948.

[10] L. Néel, “Théorie du trainage magnétique des ferromagnétiques au grains fin avec applications aux terres cuites,” *Ann. Géophys*. vol.5, pp. 99–136, Jan. 1949.

[11] G. F. Goya *et al.* “Static and dynamic magnetic properties of spherical magnetite nanoparticles,” *J. Appl. Phys*. vol. 94, pp. 3520-3529, Aug. 2003.

[12] R. Yanes *et al.,* “Effective anisotropies and energy barriers of magnetic nanoparticles with Néel surface anisotropy,” *Phys. Rev. B* vol. 76, Aug. 2007.

[13] R. Perzynski and Y. Raikher, “Effect of surface anisotropy on the magnetic resonance properties of nanosize ferroparticles,” In: Fiorani D. (eds) Surface Effects in Magnetic Nanoparticles. Nanostructure Science and Technology. Springer, Boston, MA, 2005.

[14] F. Bodker *et al.,* “Surface effects in metallic iron nanoparticles,” *Phys. Rev. Lett.* vol. 72, 282, Jan. 1994.

References

[15] C. P. Wen, “Coplanar waveguide: a surface strip transmission line suitable for nonreciprocal gyromagnetic device applications,” *IEEE Trans. Microw. Theory Techn.,”* vol. MTT-17, no. 12, pp. 1087-1090, Dec. 1969.

[16] https://getbondic.io/offer-01/

[17] J. Leliaert *et al.,* “Vinamax: a macrospin simulation tool for magnetic nanoparticles,” *Med. Biol. Eng. Comput.* Vol. 53, pp. 309-317, Jan. 2015.

[18] https://ferrofluid.ferrotec.com/products/ferrofluid-emg/water/emg-700-sp/

[19] D. I. Santiago-Quinones *et al.,* “A comparison of the magnetorheology of two ferrofluids with different magnetic field-dependent chaining behavior,” *Rheol. Acta,* vol. 52, pp. 719-726, 2013.

[20] V. M. Buzmakov and A. F. Pshenichnikov, “On the structure of microaggregates in magnetite colloids,” *J. Colloid Interface Sci.*, vol. 182, no. 0437, pp. 63-70, Mar. 1996.

[21] J. Popplewell, *et al.,* “Chain formation in magnetic fluid composites,” *IEEE Trans. Magn.*, vol. MAG-22, no. 5, pp. 1128-1130, Sept. 1986.

References

[22] J. D. Jackson, “Magnetostatics, Faraday’s Law, Quasi-Static Fields,” in *Classical Electrodynamics*, 3rd ed. New York, Wiley, 1999, Ch. 5, sec. 5.6, p. 186.

[23] E. Lima, Jr. *et al.,* “Surface effects in the magnetic properties of crystalline 3 nm ferrite nanoparticles chemically synthesized,” *J. Appl. Phys*. vol. 108, p. 103919-1-103919-10, Nov. 2010.

[24] K. Gilmore, *et al.,* “Surface contribution to the anisotropy energy of spherical magnetite particles,” *J. Appl. Phys.* vol. 97, 10B301, May 2005.

[25] L. Néel, “Anisotropie magnétique superficielle et surstructures d’orientation,” *J. Phys. Radium* vol. 15, no. 4, pp. 225-239, Apr. 1954.

[26] A. O. Ivanov, “The aggregation of ferrocolloids in a magnetic field,” *Colloid Journal*, vol. 66, no. 6, pp. 766-774, 2004.

[27] R. Montazeri and P. Zamankhan, “Two and three dimensional Monte Carlo simulation of magnetite nanoparticle based ferrofluids,” *Int. J. Eng. IJE Trans. A: Basics*, vol. 26, no. 1, pp. 99-104, Jan. 2013.